

## Theoretical Studies of Competing Reaction Pathways and Energy Barriers for Alkaline Ester Hydrolysis of Cocaine

Chang-Guo Zhan<sup>\*,†</sup> and Donald W. Landry<sup>\*</sup>

Department of Medicine, College of Physician & Surgeons, Columbia University, New York, New York 10032

Received: June 27, 2000; In Final Form: September 26, 2000

Reaction pathways, solvent effects, and energy barriers have been determined for the base-catalyzed hydrolysis of the benzoyl-ester and methyl-ester groups of neutral cocaine and three smaller alkyl esters in aqueous solution by performing a series of ab initio molecular orbital and density functional theory calculations. The reaction coordinate calculations indicate that both the benzoyl-ester hydrolysis and the methyl-ester hydrolysis occur through a two-step process known for the majority of alkyl esters, i.e., the formation of a tetrahedral intermediate by the attack of hydroxide oxygen at the carbonyl carbon (first step) followed by the decomposition of the tetrahedral intermediate to products (second step). This is the first first-principles study of the whole reaction pathway for cocaine benzoyl- and methyl-ester hydrolyses. The decomposition of the tetrahedral intermediate requires a proton transfer from the hydroxide/hydroxyl oxygen to the ester oxygen, as the C–O bond between carbonyl carbon and ester oxygen gradually breaks. We have examined two competing pathways for the second step of cocaine hydrolysis: one associated with the direct proton transfer from the hydroxide/hydroxyl oxygen to the ester oxygen, and the other associated with a water-assisted proton transfer. The energy barriers calculated for the second step of the benzoyl- and methyl-ester hydrolyses with water-assisted proton transfer are lower than the first step, whereas with direct proton transfer the barrier for the second step is higher. The first step should be rate-determining for the hydrolysis of both esters in aqueous solution, thus providing theoretical support to the design of the analogues of the first transition state that elicited anti-cocaine catalytic antibodies. The energy barrier, 7.6 kcal/mol, calculated for the first step of benzoyl-ester hydrolysis through the hydroxide attack from the Re face of the carbonyl is  $\sim 1$  kcal/mol lower than that through the hydroxide attack from the Si face. The energy barrier, 7.0 kcal/mol, calculated for the first step of cocaine methyl-ester hydrolysis is slightly lower than that of the benzoyl-ester. The effect of substituents on this energy barrier suggests that the transition state is significantly stabilized by hydrogen bonding between the hydroxide oxygen and the  $\beta$  hydrogen for the carboxylic acid or alcohol moiety.

### Introduction

Cocaine has been used by over 40 million Americans since 1980 and addiction afflicts about 2 million, with disastrous medical and social consequences.<sup>1,2</sup> This widely abused drug, which reinforces self-administration in relation to the peak serum concentration of the drug, the rate of rise to the peak, and the degree of change of the serum level, produces potent central nervous system and cardiovascular stimulation followed by depression.<sup>3</sup> With overdose of the drug, respiratory depression, cardiac arrhythmia, and acute hypertension are common effects.<sup>4</sup> Despite extensive efforts utilizing a classical approach that seeks small molecules to interfere with the cocaine-receptor interaction-(s),<sup>3a</sup> no antagonist to the reinforcing or toxic effects of cocaine has been identified. An alternative to receptor-based approaches is to interfere with the delivery of cocaine to the central nervous system and speed up its clearance from the body.<sup>3f</sup> For this purpose, we developed anti-cocaine catalytic antibodies with the capacity to bind and degrade cocaine.<sup>5</sup> This novel class of artificial enzymes was elicited by immunization with transition-state analogues of cocaine benzoyl-ester hydrolysis.

Generally speaking, design of a transition-state analogue employed to elicit a catalytic antibody<sup>6</sup> is based on the mechanism

of the corresponding nonenzymatic reaction, especially the transition state structure for the rate-determining step. Hence, a more complete understanding of the mechanisms of cocaine hydrolysis could provide additional insights into the rational design of the transition-state analogues to elicit more active monoclonal antibodies capable of catalyzing cocaine hydrolysis.

Alkaline hydrolysis of the majority of common alkyl esters, RCOOR', occurs by the attack of hydroxide ion at the carbonyl carbon.<sup>7</sup> This mode of hydrolysis has been designated as B<sub>AC</sub>2 (base-catalyzed, acyl-oxygen cleavage, bimolecular),<sup>7c</sup> and is believed to occur by a two-step mechanism, although a concerted pathway can arise in the case of esters containing very good leaving groups (corresponding to a low pK<sub>a</sub> value for R'OH).<sup>8</sup> The generally accepted two-step mechanism consists of the formation of a tetrahedral intermediate (first step), followed by decomposition of the tetrahedral intermediate to yield products RCOO<sup>-</sup> + R'OH (second step).<sup>7c</sup> Degradation of cocaine may take place through the B<sub>AC</sub>2 route of hydrolysis of either the benzoyl-ester group or the methyl-ester group.

Previous theoretical calculations of cocaine hydrolysis focused on the first step of the hydrolysis of the benzoyl-ester.<sup>9</sup> MNDO, AM1, PM3, and SM3 semiempirical molecular orbital methods, as well as an ab initio procedure at the HF/3-21G level of theory, were employed to optimize geometries of the transition states for the first step of the hydrolysis of cocaine and model esters,

<sup>†</sup> Currently visiting at Pacific Northwest National Laboratory, Mailstop K1-83, Battelle Blvd., P. O. Box 999, Richland, WA 99352. E-mail: Chang-Guo.Zhan@pnl.gov.

including methyl acetate,<sup>10</sup> for which experimental activation energy in aqueous solution is available. The geometry optimization of the first transition state for the cocaine benzoyl-ester hydrolysis was successful with only the MNDO, PM3, and SM3 methods. No first-order saddle point corresponding to the expected transition state structure was found on the AM1 and HF/3-21G potential energy surfaces. Thus, it is necessary to further examine this putative transition state with higher levels of theory. Further, the energy barrier, 24.6 kcal/mol,<sup>9a</sup> predicted by the semiempirical molecular orbital calculations for the first step of the hydrolysis of neutral cocaine in aqueous solution is likely overestimated, because the energy barrier, 23.4 kcal/mol,<sup>10</sup> determined by the same kind of calculations for the first step of the methyl acetate hydrolysis was significantly larger than the reported experimental activation energy, 10.45 kcal/mol<sup>11</sup> or 12.2 kcal/mol,<sup>12</sup> in aqueous solution.

No theoretical calculation has been reported on the second step of the cocaine benzoyl-ester hydrolysis, and therefore the relative energy barriers for the two steps have not previously been compared to determine the rate-determining step of the cocaine benzoyl-ester hydrolysis. Furthermore, the reaction pathway for the hydrolysis of the cocaine methyl-ester has not previously been subjected to calculation. In the absence of this result, the pathways and the corresponding energy barriers for the two competing reactions of cocaine remain to be compared.

We attempt herein to examine the entire reaction pathways for the hydrolysis of both the benzoyl-ester and methyl-ester groups of neutral cocaine and to predict the corresponding energy barriers with first-principles calculations. A series of ab initio and density functional theory (DFT) calculations were carried out on the hydrolysis of cocaine and three model esters. The energy barriers determined for the cocaine hydrolysis are compared with those calculated for the hydrolysis of the other esters to evaluate substituent effects on hydrolysis.

### Calculation Methods

Geometries of all transition states, reactants, and intermediates considered in this study were first optimized at the HF/3-21G and HF/6-31G levels of theory, and then refined by using Becke's three parameter hybrid exchange functional<sup>13</sup> and the Lee–Yang–Parr correlation functional (B3LYP)<sup>14</sup> with the 6-31+G(d) basis set. Vibrational frequencies were evaluated at the optimized geometries to confirm all of the first-order saddle points and local minima found on the potential energy surfaces, and to evaluate zero-point vibration energies (ZPVE). Intrinsic reaction coordinate (IRC) calculations<sup>15</sup> were also performed to verify the expected connections of the first-order saddle points with local minima found on the potential energy surfaces. The geometries optimized at the B3LYP/6-31+G(d) level were employed to carry out the single-point energy calculations at the MP2/6-31+G(d) level. Numerical results obtained for the base-catalyzed hydrolysis of methyl acetate in gas phase indicate that the B3LYP/6-31+G(d) geometry optimization followed by the MP2/6-31+G(d) single-point energy calculation is adequate for studying the energy profile of the ester hydrolysis.<sup>16</sup> Further tests indicate that the energy change from the individual reactants, methyl acetate and hydroxide, to the first transition state calculated at the MP2/6-31+G(d)//B3LYP/6-31+G(d) level is  $\sim 0.3$  kcal/mol larger than that calculated at the MP2/6-31++G(d,p)//B3LYP/6-31++G(d,p) level.

Solvent shifts of the energies were accounted for by performing self-consistent reaction field (SCRF) energy calculations using the geometries optimized at the B3LYP/6-31+G(d) level

in gas phase. The energy barrier for reaction in aqueous solution was taken as a sum of the energy change calculated at the MP2/6-31+G(d)//B3LYP/6-31+G(d) level in gas phase and the corresponding solvent shift determined by the SCRF calculations at the HF/6-31+G(d) level.

The solute–solvent interaction can be divided into a long-range electrostatic interaction and short-range nonelectrostatic interactions (such as cavitation, dispersion, and Pauli repulsion).<sup>17</sup> The dominant long-range electrostatic interaction was evaluated by using the recently developed GAMESS<sup>18</sup> implementation of the surface and volume polarization for electrostatic interactions (SVPE).<sup>19</sup> The SVPE model was sometimes also called the fully polarizable continuum model (FPCM)<sup>20,21</sup> because it fully accounts for both surface and volume polarization effects in the SCRF calculation. Because the solute cavity surface is defined as a solute electron charge isodensity contour determined self-consistently during the SVPE iteration process, the SVPE results, converged to the exact solution of Poisson's equation with a given numerical tolerance, depend only on the contour value at a given dielectric constant and a certain quantum chemical calculation level.<sup>19</sup> By seeking the best overall agreement with experimental conformational free energy differences (62 experimental observations) in various polar solutes existing in various solvents, this single parameter value has been calibrated as  $\sim 0.001$  au.<sup>19b</sup> By seeking the best overall agreement with experimental <sup>15</sup>N NMR chemical shifts (48 experimental observations) in various polar solutes existing in various solvents, this single parameter value has been calibrated as  $\sim 0.002$  au.<sup>19c</sup> Nevertheless, for both the experimental conformational free energy differences and the NMR chemical shifts, the SVPE results with the 0.002 au contour are very close to the corresponding SVPE results with the 0.001 au contour. Based on the fitting process employed in the calibration,<sup>19b</sup> the root-mean-squares (rms) deviations of the 62 experimental values for the conformational free energy differences from the results calculated by SVPE method using the 0.001 and 0.002 au contours are 0.096 and 0.104 kcal/mol, respectively. The rms deviations of the 48 experimental values for the NMR chemical shifts from the results calculated by the SVPE method using the 0.001 and 0.002 au contours are 2.6 and 2.3 ppm, respectively.<sup>19c</sup> Obviously, the 0.001 and 0.002 au contours are all acceptable for the SVPE calculations on the both kinds of properties. Recent SVPE calculations<sup>22</sup> on the base-catalyzed hydrolysis of a series of carboxylic acid esters indicated that the energy barriers determined by the SVPE calculations using both the 0.001 and 0.002 au contours are all qualitatively consistent with the corresponding experimental activation energies. The SVPE calculations using the 0.001 au contour slightly and systematically underestimate the energy barriers, whereas the differences between values from the SVPE calculations using the 0.002 au contour and the corresponding average experimental values for the examined esters are smaller than the range of experimental values reported by different laboratories. Besides, Bentley recently employed the minimum in the electron density function between pairs of interacting molecules to estimate molecular sizes and found that the molecular surfaces identified by such a procedure are in excellent agreement with the 0.002 au isodensity contour.<sup>23</sup> So, the 0.002 au contour was used in this study.

Finally, the contributions of short-range nonelectrostatic interactions to the energy barriers were estimated by using the polarizable continuum model (PCM)<sup>24</sup> implemented in the Gaussian 98 program<sup>25</sup> with the default choices of the program for the recommended standard parameters. The total solvent shift

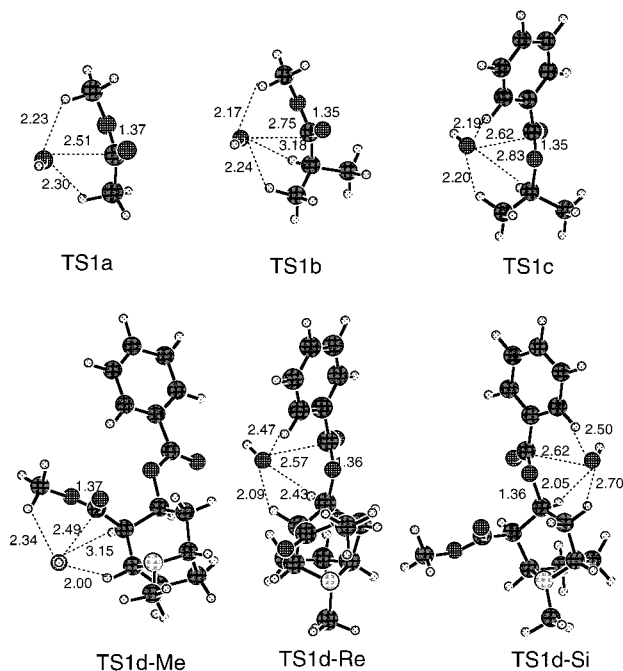


**Figure 1.** Geometries of the transition states optimized at the B3LYP/6-31+G(d) level for the first step of the hydrolysis of  $\text{CH}_3\text{COOCH}_3$ ,  $(\text{CH}_3)_2\text{CHCOOCH}_3$ ,  $\text{C}_6\text{H}_5\text{COOCH}(\text{CH}_3)_2$ , the cocaine methyl-ester, and the cocaine benzoyl-ester. The internuclear distances are given in angstrom.

was a sum of the long-range electrostatic interaction contribution determined by the SVPE calculations and the total contribution of the short-range nonelectrostatic interactions determined by the PCM calculations.

Unless otherwise indicated, the Gaussian 94<sup>26</sup> and Gaussian 98<sup>25</sup> programs were used to obtain the present results. All of the calculations in this work were performed on Silicon Graphics, Inc. Origin 200 multiprocessor computers.

## Results and Discussion

**Geometries of Transition States and Intermediates.** The important geometries optimized at the B3LYP/6-31+G(d) level for the base-catalyzed hydrolysis of neutral cocaine and three model esters are depicted in Figures 1 and 2. Note that throughout this paper the suffix “a” refers to  $\text{CH}_3\text{COOCH}_3$ , “b” refers to  $(\text{CH}_3)_2\text{CHCOOCH}_3$ , “c” refers to  $\text{C}_6\text{H}_5\text{COOCH}(\text{CH}_3)_2$ , and “d” refers to cocaine. The reaction coordinate calculations indicate that the mechanisms of the base-catalyzed hydrolysis of the cocaine benzoyl-ester and methyl-ester groups are similar to the usual two-step  $\text{B}_{\text{AC}}2$  route of hydrolysis of alkyl esters.<sup>7c,16</sup> The first step is the formation of a tetrahedral intermediate by the attack of hydroxide oxygen at the carbonyl carbon of cocaine methyl-ester or benzoyl-ester group. The second step is the decomposition of the tetrahedral intermediate to products through breaking of the C–O bond between the carbonyl carbon and ester oxygen.

For the cocaine benzoyl-ester hydrolysis, the nucleophilic hydroxide ion can approach from the two faces, denoted by Re and Si, of the carbonyl to form two stereoisomer tetrahedral intermediates (*S* and *R*). The two transition state structures, denoted by TS1d-Re and TS1d-Si, optimized at the B3LYP/6-31+G(d) level for the two competing pathways of the first step of the cocaine benzoyl-ester hydrolysis are depicted in Figure 1, together with those optimized for the first step of the hydrolysis of  $\text{CH}_3\text{COOCH}_3$  (TS1a),  $(\text{CH}_3)_2\text{CHCOOCH}_3$  (TS1b),  $\text{C}_6\text{H}_5\text{COOCH}(\text{CH}_3)_2$  (TS1c), and the cocaine methyl-ester

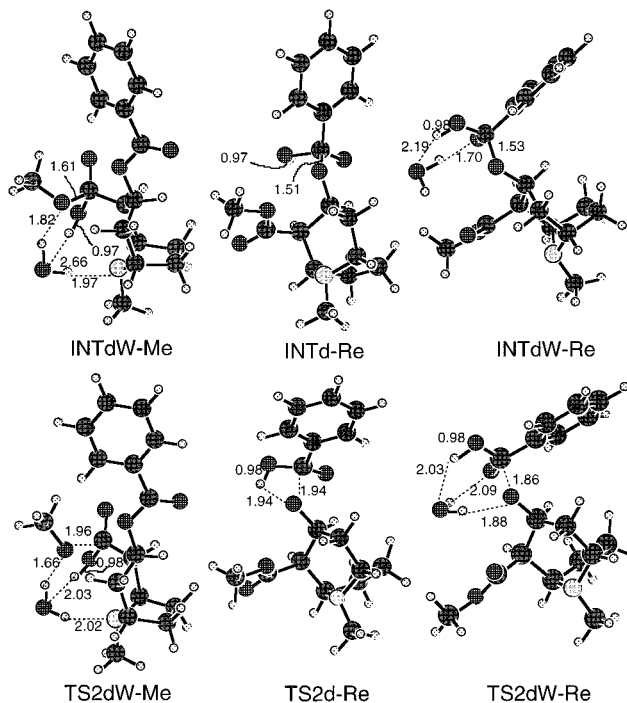


**Figure 2.** Geometries of the second transition states and the corresponding tetrahedral intermediates optimized at the B3LYP/6-31+G(d) level for the hydrolysis of the cocaine methyl-ester and benzoyl-ester groups. The internuclear distances are given in angstrom.

(TS1d-Me). As one can see from Figure 1, all of the six transition state structures for the first step are very similar to each other as far as the position of the nucleophilic hydroxide relative to the carbonyl. The distances between the hydroxide oxygen and carbonyl carbon are 2.49–2.75 Å.

As the second step of the ester hydrolysis, the decomposition of the tetrahedral intermediate requires a proton transfer from the hydroxide/hydroxyl oxygen to the ester oxygen, while the C–O bond between the carbonyl carbon and ester oxygen gradually breaks. We examined two competing pathways for the second step: one associated with the direct proton transfer from the hydroxide/hydroxyl oxygen to the ester oxygen, and the other associated with a water-assisted proton transfer. Depicted in Figure 2 are the optimized geometries of the transition state for the water-assisted proton transfer (TS2dW-Me) during the cocaine methyl-ester hydrolysis, and the transition states for the direct proton transfer (TS2d-Re) and water-assisted proton transfer (TS2dW-Re) during the cocaine benzoyl-ester hydrolysis initialized by the hydroxide attack from the Re face. Also depicted in Figure 2 are the optimized geometries of the tetrahedral intermediates INTd-Re and INTdW-Re corresponding to transition states TS2dW-Me, TS2d-Re, and TS2dW-Re, respectively. For the water-assisted proton-transfer pathway involving transition state TS2dW-Re (or TS2dW-Me), the water molecule hydrogen-bonding with the ester oxygen in the tetrahedral intermediate INTdW-Re (or INTdW-Me) gradually transfers a proton to the ester oxygen through the hydrogen bond, while the hydroxide/hydroxyl proton gradually transfers to the water oxygen.

**Energy Barriers for the Formation of the Tetrahedral Intermediates.** The energy barriers determined for the ester hydrolyses in aqueous solution are summarized in Table 1. The total energy of the individual reactants,  $\text{RCOOR}' + \text{HO}^-$ , in gas phase is about 14–26 kcal/mol higher than the first transition state (TS1). Previously reported theoretical studies of the alkaline hydrolysis of alkyl esters revealed that for the ester hydrolysis



**TABLE 1: Energy Barriers (in kcal/mol) Calculated for the Base-Catalyzed Hydrolysis of Neutral Cocaine and Model Esters in Aqueous Solution<sup>a</sup>**

reaction	$\Delta E$ (gas) <sup>b</sup>	solvent shift <sup>c</sup>			energy barrier
		electrostatic (SVPE)	nonelectrostatic (PCM) <sup>e</sup>	total	
CH <sub>3</sub> COOCH <sub>3</sub> reactants → TS1a	-14.31	25.15 [24.98] <sup>d</sup>	0.52	25.67	11.4 <sup>f</sup>
(CH <sub>3</sub> ) <sub>2</sub> CHCOOCH <sub>3</sub> reactants → TS1b	-14.05	20.97	1.05	22.02	8.0
C <sub>6</sub> H <sub>5</sub> COOCH(CH <sub>3</sub> ) <sub>2</sub> reactants → TS1c	-19.16	26.69	1.32	28.00	8.8
cocaine (methyl-ester) reactants → TS1d-Me	-18.68	24.81	0.84	25.65	7.0
INTdW-Me → TS2dW-Me	2.51	2.51	-0.23	2.28	4.8
cocaine (benzoyl-ester) reactants → TS1d-Re	-26.33	32.40	1.55	33.95	7.6
reactants → TS1d-Si	-22.99	30.26	1.25	31.51	8.5
INTd-Re → TS2d-Re	3.52	7.49	1.37	8.86	12.4
INTdW-Re → TS2dW-Re	2.16	1.32	-0.33	0.99	3.2

<sup>a</sup> All calculations used geometries optimized at the B3LYP/6-31+G(d) level in gas phase. <sup>b</sup> Energy change determined at the MP2/6-31+G(d)//B3LYP/6-31+G(d) level in gas phase. The ZPVE corrections were made for all of the values. <sup>c</sup> Unless otherwise indicated, the solvent shifts were determined by performing the SVPE and PCM calculations at the HF/6-31+G(d) level. <sup>d</sup> Values in brackets were determined by carrying out the SVPE calculations at the MP2/6-31+G(d) level. <sup>e</sup> Total contribution of nonelectrostatic interactions between solute and solvent. <sup>f</sup> The corresponding experimental activation energies reported for hydrolysis of CH<sub>3</sub>COOCH<sub>3</sub> in aqueous solution: 10.45 kcal/mol (ref 11); and 12.2 kcal/mol (ref 12).

in gas phase, between the individual reactants and TS1, there is a hydrogen-bonded reactant complex (denoted by HBR)<sup>16</sup> whose energy is lower than TS1. Thus, the energy barrier for the first step of the hydrolysis, i.e., the formation of the tetrahedral intermediate, in gas phase is the energy change from HBR to TS1. However, in aqueous solution various SCRF calculations gave the same qualitative result that the individual reactants are more stable than both TS1 and HBR, while HBR is still more stable than TS1.<sup>21</sup> It follows that in aqueous solution the HBR structure is not stable, and the reaction goes directly from the individual reactants to TS1. This is because the interaction between solvent water and the individual reactants is stronger than that between methyl acetate and hydroxide anion. Hence, the energy barrier for the first step of the hydrolysis in aqueous solution is the energy change from the individual solvated reactants to the solvated first transition state TS1. As shown in Table 1, the extremely large solvent shifts of the energy barriers for the first step of the ester hydrolysis are attributed mainly to the contributions of the long-range electrostatic interactions between the solutes and solvent.

As one can see from Table 1, the solvent shift determined for the first step of the hydrolysis of methyl acetate (the rate-determining step) by the SVPE calculations at the MP2/6-31+G(d) level<sup>19d</sup> differs from the shift determined at the HF/6-31+G(d) level by less than 0.2 kcal/mol. The calculated energy barrier, 11.4 kcal/mol, is in good agreement with the experimental determinations of activation energy, 10.45 or 12.2 kcal/mol, reported for the hydrolysis of methyl acetate in aqueous solution.<sup>11,12</sup>

As seen in Table 1, the energy barrier, 7.6 kcal/mol, calculated for the first step of the cocaine benzoyl-ester hydrolysis through the hydroxide attack from the Re face of the carbonyl is ~1 kcal/mol lower than that through hydroxide attack from the Si face. The energy barrier, 7.0 kcal/mol, calculated for the first step of the cocaine methyl-ester hydrolysis, is slightly lower than the lowest barrier, 7.6 kcal/mol, for the first step of the cocaine benzoyl-ester hydrolysis. The energy barriers calculated for the first step of the cocaine hydrolysis are all significantly lower than the barrier for the first step of the hydrolysis of methyl acetate. To understand the changes of the

calculated energy barriers from methyl acetate hydrolysis to cocaine hydrolysis, below we compared the cocaine hydrolysis with the hydrolysis of two other simplified cocaine models, (CH<sub>3</sub>)<sub>2</sub>CHCOOCH<sub>3</sub> and C<sub>6</sub>H<sub>5</sub>COOCH(CH<sub>3</sub>)<sub>2</sub>, representing the cocaine methyl-ester and benzoyl-ester, respectively.

Methyl acetate, CH<sub>3</sub>COOCH<sub>3</sub>, is a minimal model of the cocaine methyl-ester in which the two  $\beta$  carbon atoms for the carboxylic acid moiety of the methyl-ester are all simplified as hydrogen atoms. (CH<sub>3</sub>)<sub>2</sub>CHCOOCH<sub>3</sub> is a slightly larger model of the cocaine methyl-ester in which the two  $\beta$  carbon atoms for the carboxylic acid moiety of the cocaine methyl-ester are represented as methyl groups. Correspondingly, transition state structures TS1a and TS1b may be regarded as two simplified models of transition state structure TS1d-Me, as seen in Figure 1. The energy barrier, 8.0 kcal/mol, calculated for the (CH<sub>3</sub>)<sub>2</sub>-CHCOOCH<sub>3</sub> hydrolysis is 3.4 kcal/mol lower than that for the CH<sub>3</sub>COOCH<sub>3</sub> hydrolysis but matches cocaine methyl-ester hydrolysis very well at only 1.0 kcal/mol higher. It follows that substitution of the two  $\alpha$  hydrogen atoms in R with two methyl groups significantly decreases the energy barrier for the first step of the ester hydrolysis, and that further substitution of the  $\beta$  hydrogen for the carboxylic acid moiety slightly decreases the energy barrier. The significant decrease of the energy barrier upon the substitution of the two  $\alpha$  hydrogen atoms in R with two methyl groups may be attributed mainly to the stronger C-H...O hydrogen bond<sup>27</sup> between the hydroxide oxygen and one of the  $\beta$  hydrogen atoms in the first transition state (TS1b or TS1d-Me). The fact that the hydrogen bond with the  $\beta$  hydrogen is stronger than the hydrogen bond with the  $\alpha$  hydrogen is caused by the steric effect. In the transition state, the  $\beta$  hydrogen is sterically more favorable than the  $\alpha$  hydrogen to form a hydrogen bond with the hydroxide oxygen. Thus, (CH<sub>3</sub>)<sub>2</sub>CHCOOCH<sub>3</sub> is a reasonable model for the cocaine methyl-ester. Similarly, C<sub>6</sub>H<sub>5</sub>COOCH(CH<sub>3</sub>)<sub>2</sub> modeled the cocaine benzoyl-ester in which the two  $\beta$  carbon atoms for the alcohol moiety of the cocaine benzoyl-ester are represented as methyl groups. Correspondingly, transition state structure TS1c may be regarded as a model of transition state structure TS1d-Re. The energy barrier, 8.8 kcal/mol, calculated for the C<sub>6</sub>H<sub>5</sub>COOCH(CH<sub>3</sub>)<sub>2</sub> hydrolysis is very close to that of the

cocaine benzoyl-ester (TS1d-Re) at only 1.2 kcal/mol higher. Thus,  $C_6H_5COOCH(CH_3)_2$  is a reasonable model for the cocaine benzoyl-ester.

**Energy Barriers for the Decomposition of the Tetrahedral Intermediates.** The energy barrier for the second step of the cocaine hydrolysis, i.e., the decomposition of the tetrahedral intermediate, is the energy change from the intermediate (INT) to the second transition state (TS2), no matter whether the hydrolysis occurs in gas phase or in aqueous solution. Since the calculated energy barrier for the first step of the hydrolysis associated with transition state TS1d-Re is lower than that associated with transition state TS1d-Si, we considered the whole reaction pathway, individual reactants  $\rightarrow$  TS1d-Re  $\rightarrow$  INTd-Re  $\rightarrow$  TS2d-Re  $\rightarrow$  individual products, only for the cocaine benzoyl-ester hydrolysis involving the direct proton transfer. The energy barrier, 12.4 kcal/mol, calculated for the second step of the hydrolysis associated with transition state TS2d-Re is 4.8 kcal/mol higher than the corresponding first step. For the cocaine benzoyl-ester hydrolysis involving the water-assisted proton transfer, the calculated energy barrier, 3.2 kcal/mol, associated with transition state TS2dW-Re is 4.4 kcal/mol lower than the first step. It follows that the direct participation of the solvent water molecule in the proton-transfer process decreases the energy barrier by 9.2 kcal/mol. This is why the energy barrier for the second step of the hydrolysis involving the water-assisted proton transfer is significantly lower, while the energy barrier for the second step involving the direct proton transfer is significantly higher, than the first step. Thus, the reaction pathway involving the water-assisted proton transfer should dominate the hydrolysis in aqueous solution. Similar results were also obtained for the second step of the methyl acetate hydrolysis.<sup>21</sup>

For the second step of the cocaine methyl-ester hydrolysis involving the water-assisted proton transfer, the calculated energy barrier, 4.8 kcal/mol, associated with transition state TS2dW-Me is also lower than the corresponding first step. So, with the direct participation of the solvent water molecule in the proton-transfer process, the first step of the hydrolysis in aqueous solution should be rate-determining whether for the cocaine benzoyl-ester hydrolysis or the cocaine methyl-ester hydrolysis. This conclusion provides theoretical support to the design of the analogues of the first transition state for the cocaine benzoyl-ester hydrolysis to elicit anti-cocaine catalytic antibodies.<sup>5</sup>

## Conclusion

A series of ab initio molecular orbital and density functional theory calculations have been performed to examine the reaction pathways and the corresponding energy barriers for the alkaline hydrolysis of the cocaine benzoyl-ester and methyl-ester groups and three model esters in aqueous solution. The reaction coordinate calculations indicate that the mechanisms of the base-catalyzed hydrolysis of both the benzoyl-ester and methyl-ester groups of neutral cocaine are similar to the usual two-step  $B_{AC}2$  route of hydrolysis of alkyl esters. The first step is the formation of a tetrahedral intermediate by the attack of hydroxide oxygen at the carbonyl carbon of the cocaine methyl-ester or benzoyl-ester. The second step is the decomposition of the tetrahedral intermediate to products. The solvation calculations reveal the importance of the solvent effects on the energy barriers and indicate that the extremely large solvent shifts of the energy barriers for the first step of the ester hydrolysis are attributed mainly to the contributions of the long-range solute-solvent electrostatic interactions.

The decomposition of the tetrahedral intermediate requires a proton transfer from the hydroxide/hydroxyl oxygen to the ester

oxygen, as the C-O bond between the carbonyl carbon and ester oxygen gradually breaks. We examined two competing pathways for the second step of the cocaine hydrolysis: one associated with the direct proton transfer from the hydroxide/hydroxyl oxygen to the ester oxygen, and the other associated with a water-assisted proton transfer. For the water-assisted proton transfer pathway, the water molecule hydrogen-bonding with the ester oxygen in the tetrahedral intermediate gradually transfers a proton to the ester oxygen through the hydrogen bond, while the hydroxide/hydroxyl proton gradually transfers to the water oxygen. The energy barriers calculated for the second step of the hydrolyses of the benzoyl- and methyl-ester groups with water-assisted proton transfer are all lower than the first step, whereas with direct proton transfer, the energy barrier for the second step is higher. Thus, with the direct participation of the solvent water molecule in the proton transfer process, the first step of the hydrolysis in aqueous solution should be rate-determining for both the cocaine benzoyl-ester and methyl-ester groups. This conclusion strongly supports the design of analogues of the first transition state for benzoyl-ester hydrolysis that elicited anti-cocaine catalytic antibodies.

The energy barrier, 7.6 kcal/mol, calculated for the first step of the cocaine benzoyl-ester hydrolysis through the hydroxide attack from the Re face of the carbonyl is  $\sim$ 1 kcal/mol lower than that through the hydroxide attack from the Si face. The energy barrier, 7.0 kcal/mol, calculated for the first step of the methyl-ester hydrolysis is slightly lower than that of the benzoyl-ester.

Substituent effects on the energy barriers for the first step of the ester hydrolysis have also been discussed. The energy barrier, 11.4 kcal/mol, determined by the same level of calculations for methyl acetate, is in good agreement with the experimental activation energy, 10.45 or 12.2 kcal/mol, reported for the base-catalyzed hydrolysis of methyl acetate in aqueous solution. Substitution of the two  $\alpha$  hydrogen atoms for the carboxylic acid moiety with two methyl groups significantly decreases the energy barrier for the first step of the ester hydrolysis, and that further substitution of the  $\beta$  hydrogen slightly decreases the energy barrier. The significant decrease of the energy barrier upon the substitution of the two  $\alpha$  hydrogen atoms with two methyl groups may be attributed mainly to the stronger hydrogen bond between the hydroxide oxygen and one of the  $\beta$  hydrogen atoms in the first transition state. The  $\beta$  hydrogen is sterically more favorable than the  $\alpha$  hydrogen for hydrogen bonding with the hydroxide oxygen in the first transition state. Therefore, the energy barrier, 8.0 kcal/mol, calculated for the first step of the  $(CH_3)_2CHCOOCH_3$  hydrolysis is 3.4 kcal/mol lower than the  $CH_3COOCH_3$  hydrolysis, and is only 1.0 kcal/mol higher than the cocaine methyl-ester hydrolysis. The transition state structures TS1b and TS1d-Me are significantly stabilized by hydrogen bonding between the hydroxide oxygen and the  $\beta$  hydrogen. Similarly, the  $\beta$  hydrogen for the alcohol moiety is also sterically more favorable than the corresponding  $\alpha$  hydrogen for forming a hydrogen bond with the hydroxide oxygen in the first transition state. The energy barrier, 8.8 kcal/mol, calculated for the first step of the  $C_6H_5COOCH(CH_3)_2$  hydrolysis, is only 1.2 kcal/mol higher than the corresponding cocaine benzoyl-ester hydrolysis.

**Acknowledgment.** This work was supported by the Counterdrug Technology Assessment Center at the Office of National Drug Control Policy (D.W.L.).

## References and Notes

- (1) (a) Gawin, F. H.; Ellinwood, E. H., Jr. *N. Eng. J. Med.* **1988**, *318*, 1173. (b) Landry, D. W. *Sci. Am.* **1997**, *276*, 28.

- (2) Mets, B.; Winger, G.; Cabrera, C.; Seo, S.; Jamdar, S.; Yang, G.; Zhao, K.; Briscoe, R. J.; Almonte, R.; Woods, J. H.; Landry, D. W. *Proc. Natl. Acad. Sci. U.S.A.* **1998**, *95*, 10176.
- (3) (a) Fischman, M. W. *J. Clin. Psychiatry* **1988**, *49*, 7. (b) Bergman, J.; Madras, B. K.; Johnson, S. E.; Spealman, R. D. *J. Pharmacol. Exp. Ther.* **1989**, *251*, 150. (c) Johnson, C. E. *NIDA Res. Monogr.* **1984**, *50*, 54. (d) Washton, A.; Gold, M. *Cocaine: A Clinician's Handbook*; Guildford Press: New York, 1987. (e) Spitz, H. I.; Rosecan, J. S. Eds. *Cocaine Abuse: New Directions in Treatment and Research*; Brunner Mazel, Inc.: New York, 1987. (f) Gorelick, D. A. *Drug Alcohol Depend.* **1997**, *48*, 159.
- (4) Wilkerson, R. D. *NIDA Res. Monogr.* **1988**, *88*, 304.
- (5) (a) Landry D. W.; Zhao, K.; Yang, G. X.-Q.; Glickman, M.; Georgiadis, T. M. *Science* **1993**, *259*, 1899. (b) Yang, G.; Chun, J.; Arakawa-Uramoto, H.; Wang, X.; Gawinowicz, M. A.; Zhao, K.; Landry, D. W. *J. Am. Chem. Soc.* **1996**, *118*, 5881. (c) Li, P.; Zhao, K.; Deng, S.; Landry, D. W. *Helv. Chim. Acta* **1999**, *82*, 85.
- (6) Lerner, R. A.; Benkovic, S. J.; Schultz, P. G. *Science* **1991**, *252*, 659.
- (7) (a) Jones, R. A. Y. *Physical and Mechanistic Organic Chemistry*; Cambridge University Press: Cambridge, 1979; p 227. (b) McMurry, J. *Organic Chemistry*, 2nd ed.; Cole Publishing: California, 1988. (c) Lowry, T. H.; Richardson, K. S. *Mechanism and Theory in Organic Chemistry*, 3rd ed.; Harper and Row: New York, 1987. (d) Williams, A. In *Enzyme Mechanisms*; Page, M. I.; Williams, A., Eds.; Burlington: London, 1987; p 123.
- (8) (a) Bender, M. L.; Thomas, R. J. *J. Am. Chem. Soc.* **1961**, *83*, 4189. (b) Bender, M. L.; Matsui, H.; Thomas, R. J.; Tobey, S. W. *J. Am. Chem. Soc.* **1961**, *83*, 4193. (c) Bender, M. L.; Heck, H., d'A. *Ibid.* **1967**, *89*, 1211. (d) Bender, M. L.; Ginger, R. D.; Unik, J. P. *Ibid.* **1958**, *80*, 1044. (e) O'Leary, M. H.; Marlier, J. F. *J. Am. Chem. Soc.* **1979**, *101*, 3300. (f) Guthrie, J. P. *J. Am. Chem. Soc.* **1991**, *113*, 3941. (g) Hengge, A. *J. Am. Chem. Soc.* **1992**, *114*, 6575. (h) Marlier, J. F. *J. Am. Chem. Soc.* **1993**, *115*, 5953.
- (9) (a) Sherer, E. C.; Turner, G. M.; Lively, T. N.; Landry, D. W.; Shields, G. C. *J. Mol. Model.* **1996**, *2*, 62. (b) Sherer, E. C.; Yang, G.; Turner, G. M.; Shields, G. C.; Landry, D. W. *J. Phys. Chem. A* **1997**, *101*, 8526.
- (10) (a) Sherer, E. C.; Turner, G. M.; Shields, G. C. *Int. J. Quantum Chem. Quantum Biol. Symp.* **1995**, *22*, 83. (b) Turner, G. M.; Sherer, E. C.; Shields, G. C. *Int. J. Quantum Chem. Quantum Biol. Symp.* **1995**, *22*, 103.
- (11) Fairclough, R. A.; Hinshelwood, C. N. *J. Chem. Soc.* **1937**, 538.
- (12) Rylander, P. N.; Tarbell, D. S. *J. Am. Chem. Soc.* **1950**, *72*, 3021.
- (13) Becke, A. D. *J. Chem. Phys.* **1993**, *98*, 5648.
- (14) Lee, C.; Yang, W.; Parr, R. G. *Phys. Rev. B* **1988**, *37*, 785.
- (15) (a) Gonzalez, C.; Schlegel, H. B. *J. Chem. Phys.* **1989**, *90*, 2154. (b) Gonzalez, C.; Schlegel, H. B. *J. Phys. Chem.* **1990**, *94*, 5523.
- (16) Zhan, C.-G.; Landry, D. W.; Ornstein, R. L. *J. Am. Chem. Soc.* **2000**, *122*, 1522.
- (17) (a) Tomasi, J.; Persico, M. *Chem. Rev.* **1994**, *94*, 2027. (b) Cramer, C. J.; Truhlar, D. G. In *Solvent Effects and Chemical Reactions*; Tapia, O., Bertran, J., Eds.; Kluwer: Dordrecht, 1996; p 1. (c) Cramer, C. J.; Truhlar, D. G. *Chem. Rev.* **1999**, *99*, 2161. (d) Chipman, D. M. *J. Chem. Phys.* **1997**, *106*, 10194. (e) Chipman, D. M. *J. Chem. Phys.* **1999**, *110*, 8012.
- (18) Schmidt, M. W.; Baldrige, K. K.; Boatz, J. A.; Elbert, S. T.; Gordon, M. S.; Jensen, J. H.; Koseki, S.; Matsunaga, N.; Nguyen, K. A.; Su, S. J.; Windus, T. L.; Dupuis, M.; Montgomery, J. A. *J. Comput. Chem.* **1993**, *14*, 1347.
- (19) (a) Zhan, C.-G.; Bentley, J.; Chipman, D. M. *J. Chem. Phys.* **1998**, *108*, 177. (b) Zhan, C.-G.; Chipman, D. M. *J. Chem. Phys.* **1998**, *109*, 10543. (c) Zhan, C.-G.; Chipman, D. M. *J. Chem. Phys.* **1999**, *110*, 1611. (d) For the SVPE calculations with the MP2 method, the MP2 perturbation procedure was performed for electron correlation correction after the converged HF wave function of solute in reaction field is obtained. (e) Regarding the detail of the SVPE computation on a given solute under a given quantum mechanical approximation level, once the solute cavity is defined and the dielectric constant is known, the accuracy of the SVPE numerical computation depends only on the number of surface nodes ( $N$ ) representing the cavity surface and number of layers ( $M$ ) describing the volume polarization charge distribution within a certain, sufficiently large three-dimensional space outside the solute cavity. If one could use an infinite number of nodes and an infinite number of layers, then the numerical results obtained from the SVPE computation would be exactly the same as those determined by the exact solution of the Poisson's equation for describing the solvent polarization potential. We have shown that the accuracy of the SVPE numerical computations employed in this study with  $N = 590$  and  $M = 40$  (for a step of 0.3 Å) are higher than what are required for listing Table 1 in this paper. The dielectric constant of water used for the SVPE calculations is 78.5.
- (20) Zhan, C.-G.; Norberto de Souza, O.; Rittenhouse, R.; Ornstein, R. L. *J. Am. Chem. Soc.* **1999**, *121*, 7279.
- (21) Zhan, C.-G.; Landry, D. W.; Ornstein, R. L. *J. Am. Chem. Soc.* **2000**, *122*, 2621.
- (22) Zhan, C.-G.; Landry, D. W.; Ornstein, R. L. *J. Phys. Chem. A* **2000**, *104*, 7672.
- (23) Bentley, J. *J. Phys. Chem. A* **1998**, *102*, 6043.
- (24) (a) Miertus, S.; Scrocco, E.; Tomasi, J. *Chem. Phys.* **1981**, *55*, 117. (b) Miertus, S.; Tomasi, J. *Chem. Phys.* **1982**, *65*, 239. (c) Cossi, M.; Barone, V.; Cammi, R.; Tomasi, J. *Chem. Phys. Lett.* **1996**, *255*, 327.
- (25) Frisch, M. J.; Trucks, G. W.; Schlegel, H. B.; Scuseria, G. E.; Robb, M. A.; Cheeseman, J. R.; Zakrzewski, V. G.; Montgomery, J. A.; Stratmann, R. E.; Burant, J. C.; Dapprich, S.; Millam, J. M.; Daniels, A. D.; Kudin, K. N.; Strain, M. C.; Farkas, O.; Tomasi, J.; Barone, V.; Cossi, M.; Cammi, R.; Mennucci, B.; Pomelli, C.; Adamo, C.; Clifford, S.; Ochterski, J.; Petersson, G. A.; Ayala, P. Y.; Cui, Q.; Morokuma, K.; Malick, D. K.; Rabuck, A. D.; Raghavachari, K.; Foresman, J. B.; Cioslowski, J.; Ortiz, J. V.; Stefanov, B. B.; Liu, G.; Liashenko, A.; Piskorz, P.; Komaromi, I.; Gomperts, R.; Martin, R. L.; Fox, D. J.; Keith, T.; Al-Laham, M. A.; Peng, C. Y.; Nanayakkara, A.; Gonzalez, C.; Challacombe, M.; Gill, P. M. W.; Johnson, B.; Chen, W.; Wong, M. W.; Andres, J. L.; Gonzalez, A. C.; Head-Gordon, M.; Replogle, E. S.; Pople, J. A. *Gaussian 98*, Revision A.6, Gaussian, Inc.: Pittsburgh, PA, 1998.
- (26) Frisch, M. J.; Trucks, G. W.; Schlegel, H. B.; Gill, P. M. W.; B. G. Johnson, B. G.; Robb, M. A.; Cheeseman, J. R.; Keith, T.; Petersson, G. A.; Montgomery, J. A.; Raghavachari, K.; Al-Laham, M. A.; Zakrzewski, V. G.; Ortiz, J. V.; Foresman, J. B.; Cioslowski, J.; Stefanov, B. B.; Nanayakkara, A.; Challacombe, M.; Peng, C. Y.; Ayala, P. Y.; Chen, W.; Wong, M. W.; Andres, J. L.; Replogle, E. S.; Gomperts, R.; Martin, R. L.; Fox, D. J.; Binkley, J. S.; Defrees, D. J.; Baker, J.; Stewart, J. P.; Head-Gordon, M.; Gonzalez, C.; Pople, J. A. *Gaussian 94*, Revision D.1, Gaussian, Inc.: Pittsburgh, PA, 1995.
- (27) (a) Gu, Y.; Kar, T.; Scheiner, S. *J. Am. Chem. Soc.* **1999**, *121*, 9411. (b) Meadows, E. S.; De Wall, S. L.; Barbour, L. J.; Fronczek, F. R.; Kim, M.-S.; Gokel, G. W. *J. Am. Chem. Soc.* **2000**, *122*, 3325. (c) Vargas, R.; Garza, J.; Dixon, D. A.; Hay, B. P. *J. Am. Chem. Soc.* **2000**, *122*, 4750.